Science Advances
AAAS

Supplementary Materials for

Physiological ROS controls Upd3-dependent modeling of ECM to support cardiac function in *Drosophila*

Jayati Gera, Prerna Budakoti, Meghna Suhag, Lolitika Mandal, Sudip Mandal*

*Corresponding author. Email: sudip@iisermohali.ac.in

Published 18 February 2022, *Sci. Adv.* **8**, eabj4991 (2022)
DOI: 10.1126/sciadv.abj4991

The PDF file includes:

Other Supplementary Material for this manuscript includes the following:

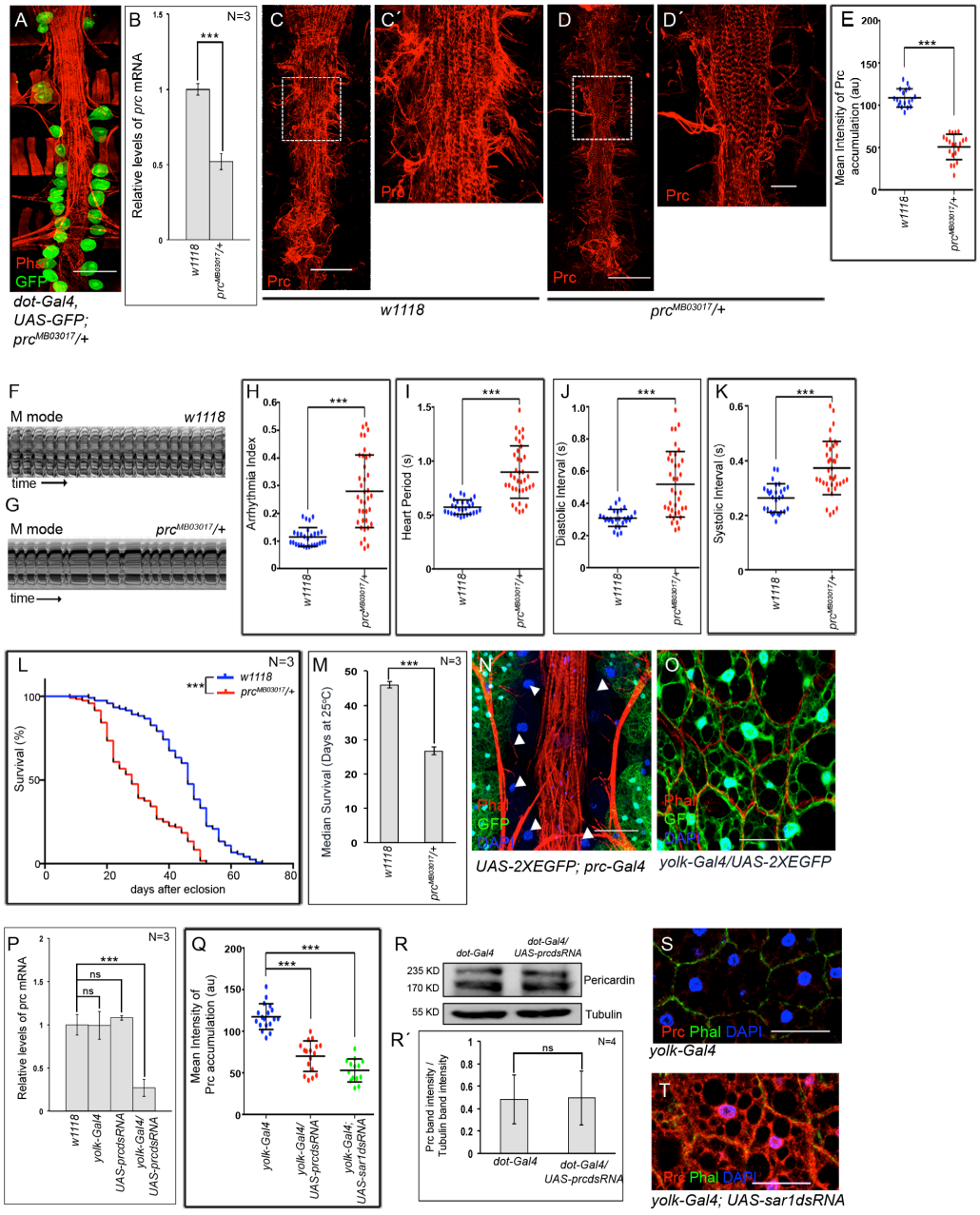

Figure S1

Figure S1: Pericardin, synthesized and released by adult fat body cells, is critical for cardiac function

(A) Heart of *prc*^{MB03017}/+ adult flies as marked with Phalloidin (red). Reporter GFP expression for *dorothy* (*dot*) marks the adult PCs. Scale = 100μ

(B) Reduction in the level of *prc* transcripts in the fat cells of *prc*^{MB03017}/+ adult flies.

(C and D′) Drop in the level of Prc (red) accumulation in the cardiac ECM of $prc^{MB03017}$/+ flies (D and D′) as compared to control (C and C′). C′ and D′ represent zoomed in image of the second heart chamber marked with a box in C and D respectively. Scale = 100μ (C and D), and 25μ (C′ and D′).

(E) Quantification of the mean fluorescence intensity for Prc accumulation around the second chamber of cardiac tube of $prc^{MB03017}$/+ flies. The dots represent the samples analyzed for each genotype.

(F and G) Representative M-mode records for heartbeats of adult flies showing the movement of the heart tube walls (y-axis) over time (x-axis).

(H - K) Changes in Arrhythmia Index (H), Heart Period (I), Diastolic Interval (J), and Systolic Interval (K) of the heart in case of $prc^{MB03017}$/+ flies. For each plot, the dots represent the samples analyzed for each genotype.

(L) Survival rates of $prc^{MB03017}$/+ flies as compared to control.

(M) Median survival of $prc^{MB03017}$/+ flies as compared to control

(N) The adult PCs (nuclei marked by arrowheads) around the cardiac tube do not exhibit reporter GFP expression for *prc*. GFP expression is observed in the surrounding fat cells. The cardiac tube and the alary muscles are marked with Phalloidin (red). DAPI (blue) marks the nuclei. Scale = 50μ

(O) Reporter GFP expression for *yolk* in the adult fat cells. The cell boundaries are marked with Phalloidin (red) and DAPI (blue) marks the nuclei. $_{\text{Scale}}$ = 50μ

(P) Reduction in the level of *prc* expression upon knocking down *prc* in adult fat cells.

(Q) Quantification of the mean fluorescence intensity for Prc accumulation around the second chamber of cardiac tube upon knocking down either *prc* or *sar1* in the fat body cells. The dots represent the samples analyzed for each genotype.

(R and R′) Western blot analysis demonstrating that the organismal Prc level remains unchanged upon knocking down *prc* in the adult PCs. The level of Tubulin serves as the loading control (R). Quantification of the Prc band intensities normalized to that of Tubulin band intensities for three independent experiments (R′).

(S and T) Knocking down of *sar1* in fat body cells leads to accumulation of Prc (red) within the fat cells (T) as compared to control (S). Phalloidin (green) marks the membrane and the nuclei are marked by DAPI (blue) Scale = 25μ.

Genotypes are as mentioned. Data are represented as mean ± SD. Statistical significance with p values of $p<0.05$, $p<0.01$, and $p<0.001$ are mentioned as *, **, and *** respectively.

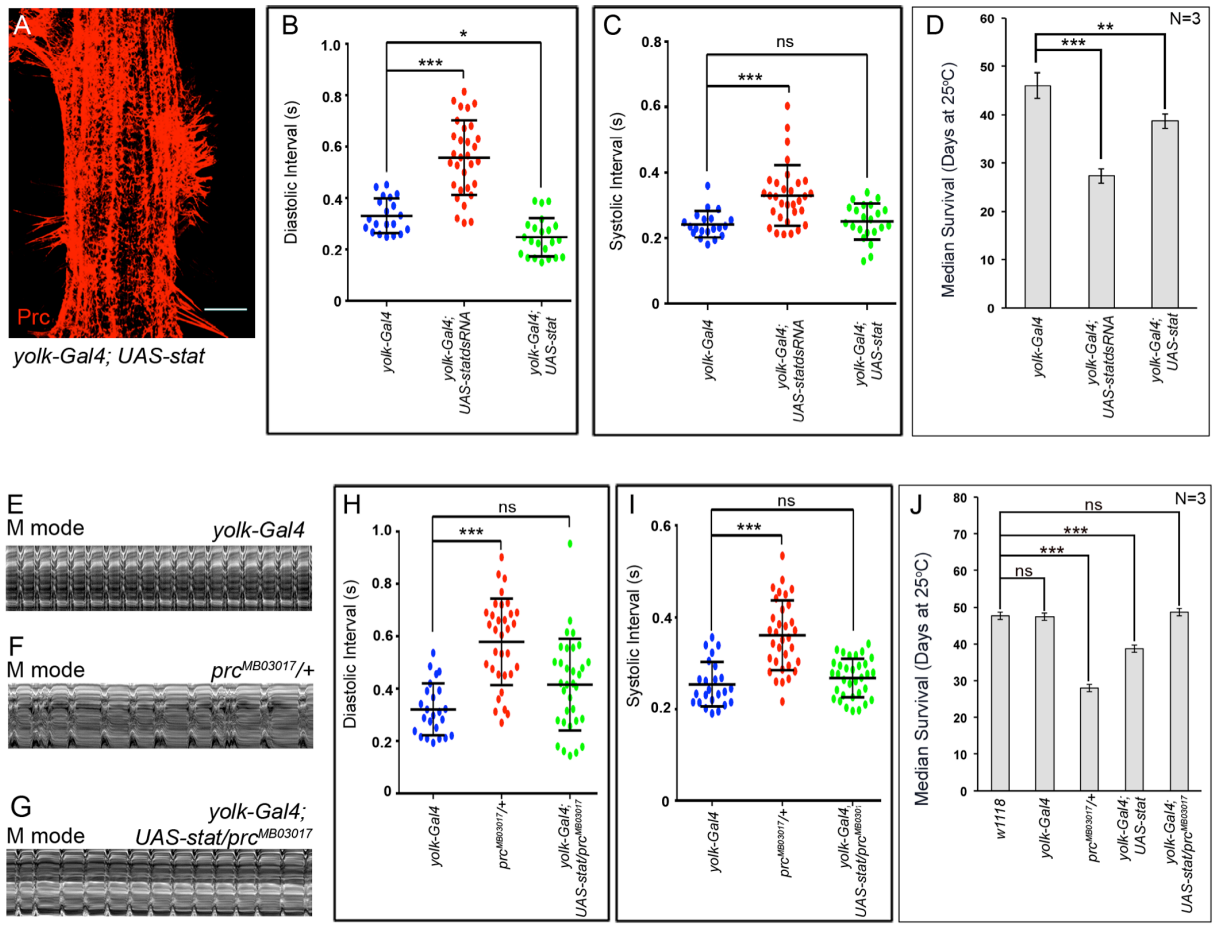

Figure S2

Figure S2: **JAK-STAT signaling regulates *prc* expression in the fat body cells**

(A) Increased Prc (red) accumulation around the second chamber of the adult heart upon over-expressing *stat92E* in fat cells. Scale = 25µ

(B and C) Changes in Diastolic Interval (B) and Systolic Interval (C) of the adult heart upon modulating JAK-STAT signaling in adult fat cells. For each plot, the dots represent the samples analyzed for each genotype.

(D) Median lifespan of the adult flies upon modulating JAK-STAT signaling in adult fat cells as compared to control.

(E – G) Representative M-mode records for heartbeats of adult flies showing the movement of the heart tube walls (y-axis) over time (x-axis).

(H - I) Rescue in Diastolic Interval (H), and Systolic Interval (I) of the heart of *prc*^{MB03017}/+ flies upon overexpression of *stat92E* in fat cells. For each plot, the dots represent the samples analyzed for each genotype.

(F-H) Rescue in the median lifespan of *prc*^{MB03017}/+ flies upon overexpression of *stat92E* in fat cells as compared to different control flies.

Genotypes are as mentioned. Data are represented as mean ± SD. Statistical significance with p values of $p<0.05$, $p<0.01$, and $p<0.001$ are mentioned as *, **, and *** respectively.

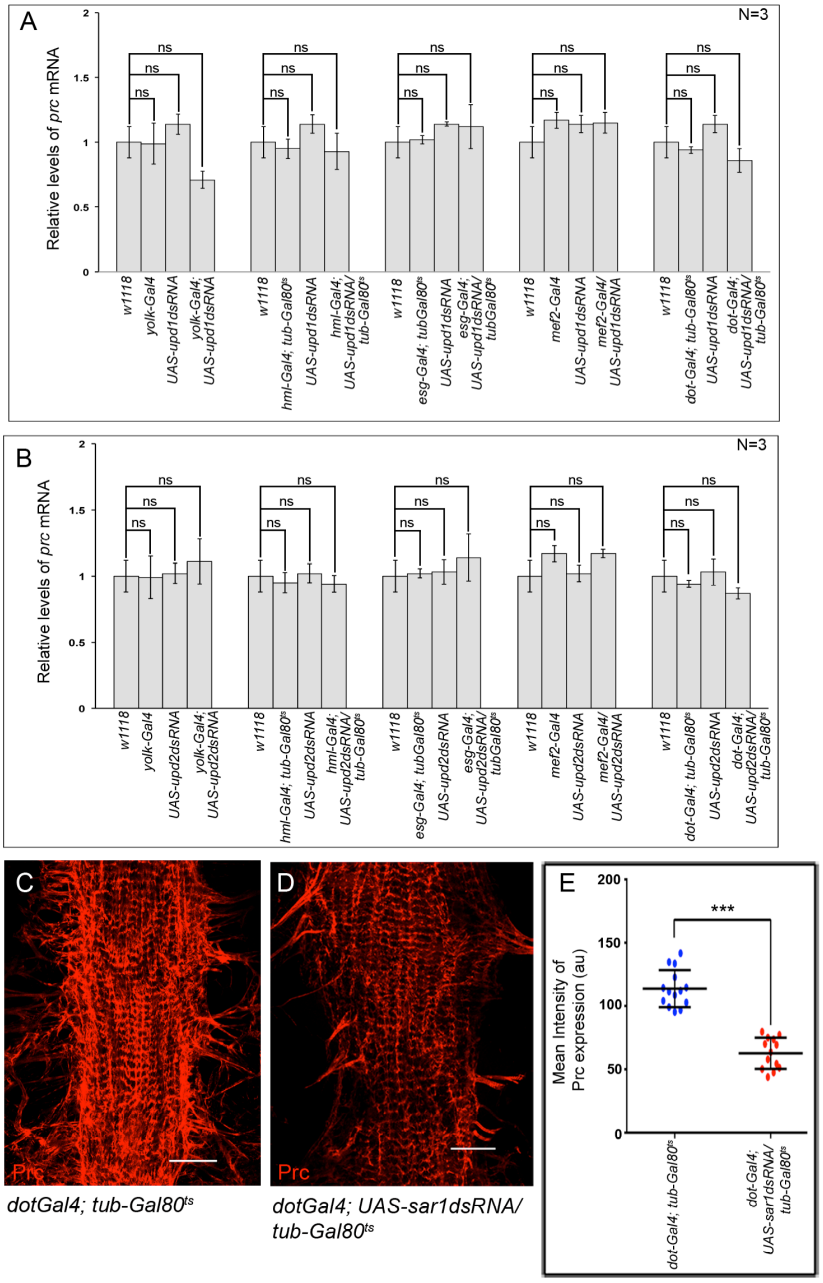

Figure S3

Figure S3: Upd3 released by PCs trigger *prc* expression in the fat body cells

(A) Levels of *prc* expression in fat cells after knocking down *upd1* from different adult tissues.

(B) Levels of *prc* expression in fat cells remain unaltered after knocking down *upd2* from different adult tissues.

(C and D) Change in Prc (red) accumulation around the second chamber of the adult heart upon downregulating *sar1* in the PCs (D) as compared to control (C). Scale = 25μ

(E) Quantification of the mean fluorescence intensity for Prc accumulation around the second chamber of the cardiac tube upon downregulating *sar1* in the PCs. The dots represent the samples analyzed for each genotype.

Genotypes are as mentioned. Data are represented as mean ± SD. Statistical significance with p values of $p<0.05$, $p<0.01$, and $p<0.001$ are mentioned as *, **, and *** respectively.

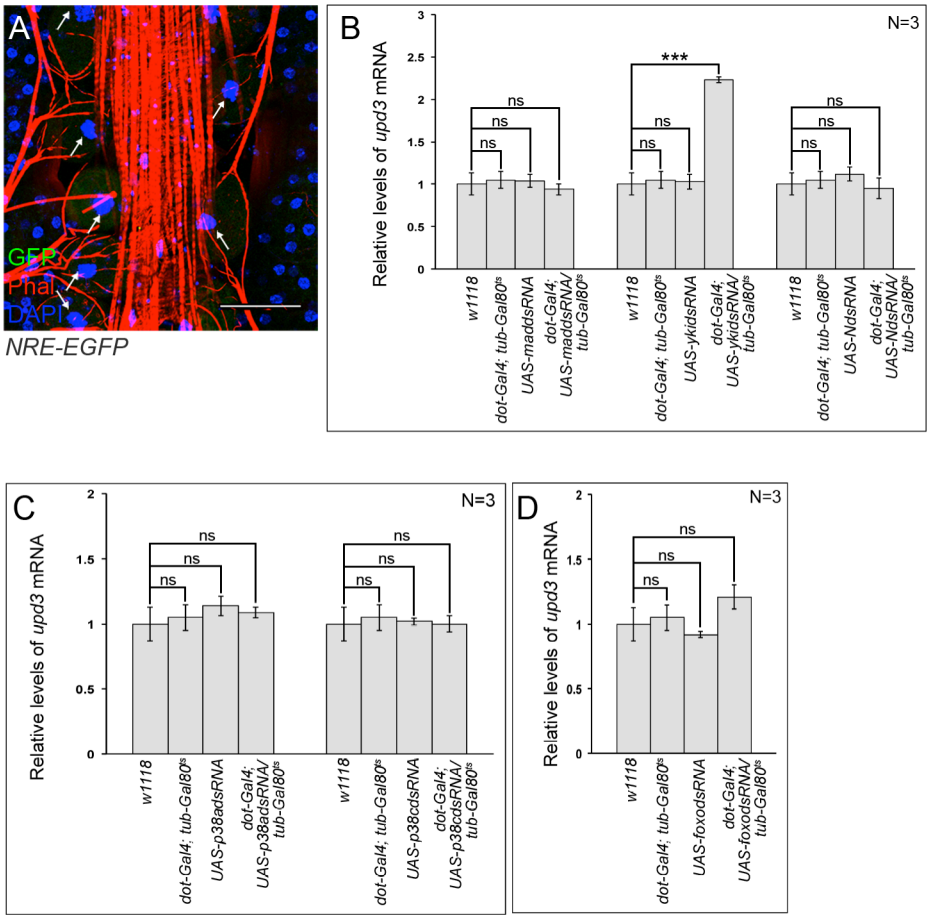

Figure S4

Figure S4: Activation of *upd3* in the pericardial cells is dependent on JNK and p38 signaling

(A) Expression of reporter GFP for *NRE* (Notch pathway) in the PCs. The cardiac tube and the alary muscles are marked with Phalloidin (red). DAPI (blue) marks the nuclei. Scale = 50μ

(B) The expression of *upd3* is not reduced upon independently knocking down *mad*, *yorkie* and *Notch* in the PCs.

(C) The expression of *upd3* remains unaltered upon independently knocking down either *p38(a)* or *p38(c)* signaling in the PCs.

(D) No change in the expression of *upd3* is observed upon knocking down *foxo* in the PCs.

Genotypes are as mentioned. Data are represented as mean ± SD. Statistical significance with p values of $p<0.05$, $p<0.01$, and $p<0.001$ are mentioned as *, **, and *** respectively.

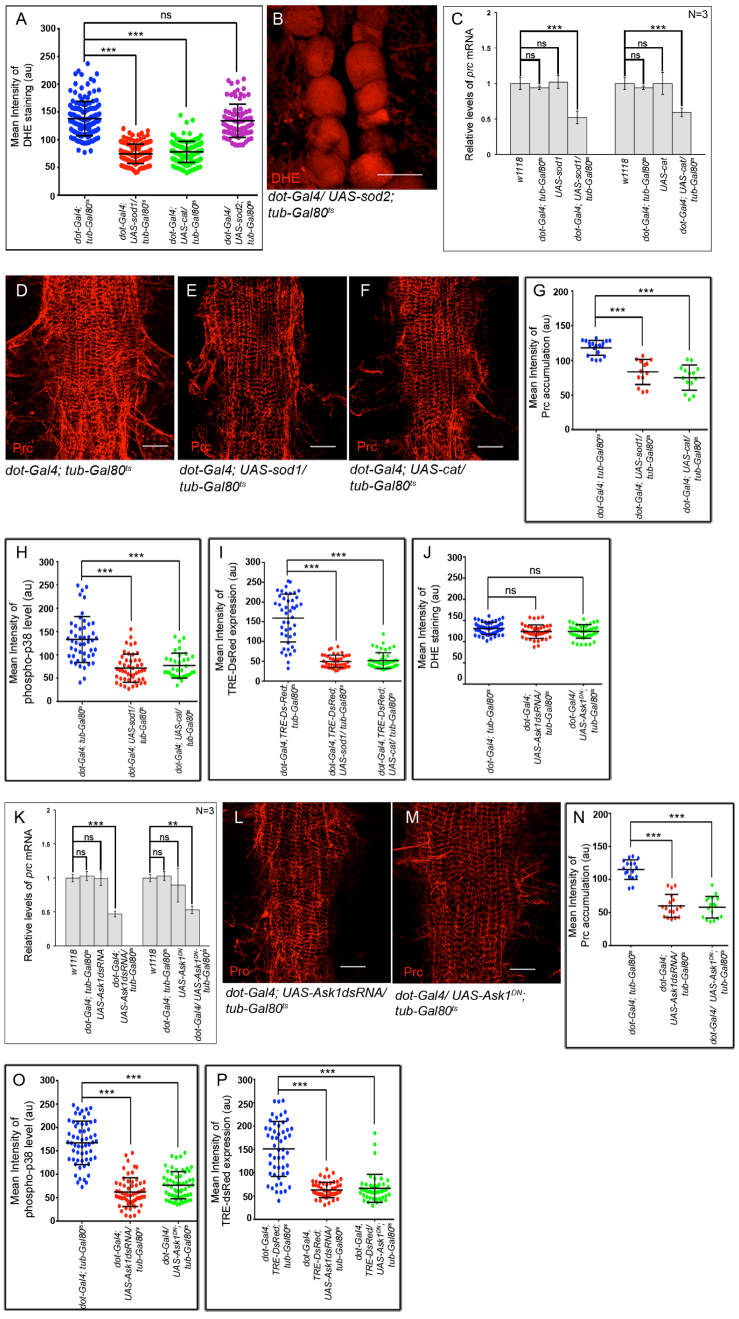

Figure S5

Figure S5: ROS dependent activation of p38 and JNK signaling in the PCs

(A) Quantification of the mean fluorescence intensity for DHE staining in the adult PCs of the genotypes mentioned. The dots represent the number of PCs analyzed for each genotype.

(B) Levels of ROS (DHE staining; red) in the PCs upon scavenging ROS by ectopic expression of SOD2. Scale = 50μ

(C) Changes in *prc* expression in the fat cells upon scavenging ROS by ectopic expression of SOD1 or Catalase in the PCs.

(D-F) Change in Prc (red) accumulation around the second chamber of the adult heart upon scavenging ROS by ectopic expression of SOD1 (E) or Catalase (F) in the PCs as compared to control (D).

(G) Quantification of the mean fluorescence intensity for Prc accumulation around the second chamber of the cardiac tube upon ectopic expression of SOD1 or Catalase in the PCs. The dots represent the samples analyzed for each genotype.

(H) Quantification of the mean fluorescence intensity for phosphorylated-p38 in the adult PCs of the genotypes mentioned. The dots represent the number of PCs analyzed for each genotype.

(I) Quantification of the mean fluorescence intensity for TRE-DsRed in the adult PCs of the genotypes mentioned. The dots represent the number of PCs analyzed for each genotype.

(J) Quantification of the mean fluorescence intensity for DHE staining in the adult PCs of the genotypes mentioned. The dots represent the number of PCs analyzed for each genotype.

(K) Changes in the level of *prc* expression in the fat cells upon attenuating *ask1* in the PCs.

(L and M) Change in Prc (red) accumulation around the second chamber of the adult heart upon attenuating *ask1* in the PCs (M) as compared to control (L).

(N) Quantification of the mean fluorescence intensity for Prc accumulation around the second chamber of the cardiac tube upon downregulating *ask1* in the PCs. The dots represent the samples analyzed for each genotype.

(O) Quantification of the mean fluorescence intensity for phosphorylated-p38 in the adult PCs of the genotypes mentioned. The dots represent the number of PCs analyzed for each genotype.

(P) Quantification of the mean fluorescence intensity for TRE-DsRed in the adult PCs of the genotypes mentioned. The dots represent the number of PCs analyzed for each genotype.

Genotypes are as mentioned. Scale = 25μ in all images (if not mentioned otherwise). Data are represented as mean ± SD. Statistical significance with p values of $p<0.05$, $p<0.01$, and $p<0.001$ are mentioned as *, **, and *** respectively.

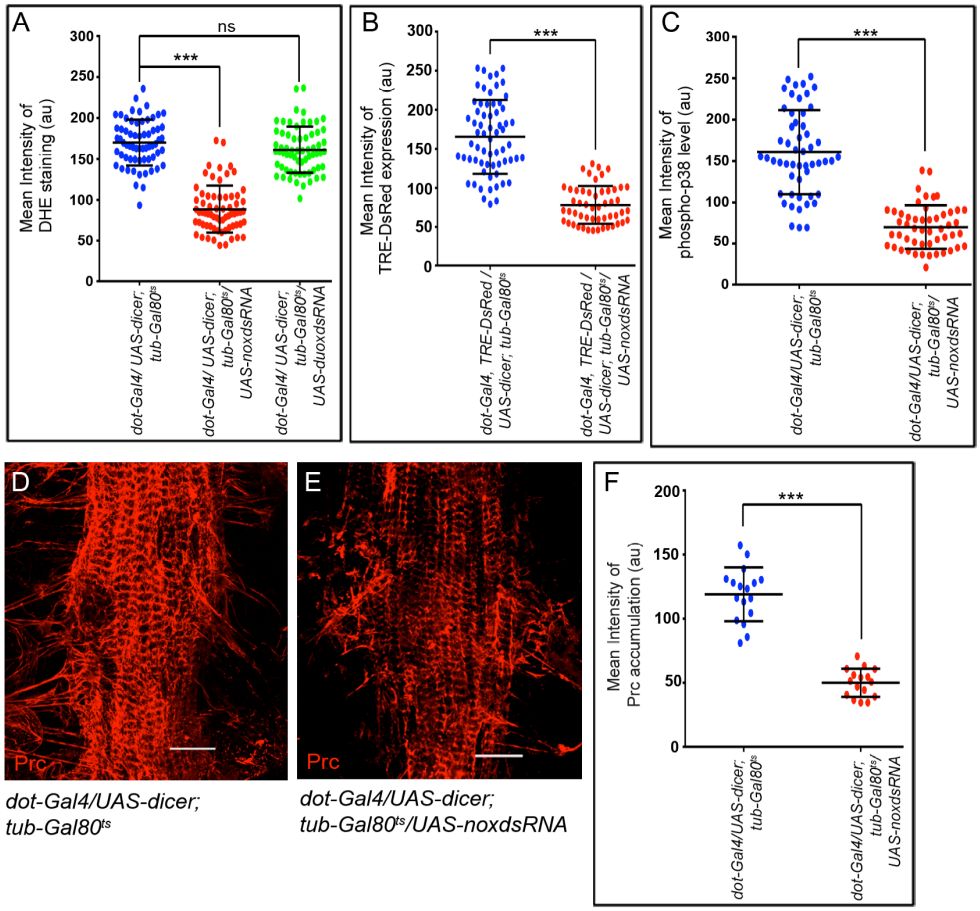

Figure S6

Figure S6: Nox activity generates elevated levels of ROS in the PCs

(A) Quantification of the mean fluorescence intensity for DHE staining in the adult PCs of the genotypes mentioned. The dots represent the number of PCs analyzed for each genotype.

(B) Quantification of the mean fluorescence intensity for TRE-DsRed in the adult PCs of the genotypes mentioned. The dots represent the number of PCs analyzed for each genotype.

(C) Quantification of the mean fluorescence intensity for phosphorylated-p38 in the adult PCs of the genotypes mentioned. The dots represent the number of PCs analyzed for each genotype.

(D and E) Change in Prc (red) accumulation around the second chamber of the adult heart upon knocking down *nox* in the PCs (E) as compared to control (D). Scale = 25μ.

(F) Quantification of the mean fluorescence intensity for Prc accumulation around the second chamber of the cardiac tube upon knocking down *nox* in the PCs. The dots represent the samples analyzed for each genotype.

Genotypes are as mentioned. Data are represented as mean ± SD. Statistical significance with p values of $p<0.05$, $p<0.01$, and $p<0.001$ are mentioned as *, **, and *** respectively.

Table S1.

Genotypes, Stock Number and the Sources of the fly lines used:

	Line	Genotype	Source
1	w^{1118}	w^{1118}	BDSC Stock# 3605
Gal4 Driver lines			
1	*dot-Gal4*	w^{1118}; *dot-Gal4*	(*62*)
2	*yolk-Gal4*	w^{1118}; *yolk-Gal4*	(*63*)
3	*mef2-Gal4*	y^{1}, w^{1118}; *P{GAL4-Mef2.R}3*	(*64*)
4	*esg-Gal4*	w^{1118}; *P{GawB}NP5130 P{UAS-GFP.U}2; P{UAS3xFLAG.dCas9.VPR} attP2 ,* $P\{tubP\text{-}GAL80^{ts}\}2$	BDSC Stock# 67072
5	*hml-Gal4*	w^{1118}; *P{Hml-GAL4.Δ}2, P{UAS-2xEGFP}AH2*	(*65*)
UAS Responder lines			
1	*UAS-2XGFP*	w^{1118}; $P\{w^{+MC}$=*UAS-2xEGFP}AH2*	BDSC Stock # 6874
2	*UAS-sodA*	w^{1118}; *P{UAS-Sod1.A}B37*	BDSC Stock# 24750
2	*UAS-sod2*	w^{1118}; *P{UAS-Sod2.M}UM83*	BDSC Stock# 24494
3	*UAS-cat*	w^{1118}; *P{UAS-Cat.A}2*	BDSC Stock# 24621
4	*UAS-*bsk^{DN}	w^{1118}, *UAS-bsk.DN*	BDSC Stock # 6409
5	*UAS-*fos^{DN}	w^{1118}; *P{UAS-Fra.Fbz}5*	BDSC Stock # 7214
6	*UAS-* $p38b^{DN}$	*P{UAS-p38b.DN}1,* w^{*}*/FM7c*	BDSC Stock # 59005
7	*UAS-p38b*	y^{1} w^{67c23}; $P\{GSV6\}p38b^{GS10799}$*/SM1*	Kyoto stock #202837
8	*UAS-* $ask1^{DN}$	w^{1118}; *P{UAS-Ask1K618M}v/Cyo*	(*66*)
9	*UAS-stat*	y^{1} w^{67c23}; $P\{EPgy2\}Stat92E^{EY14209}$*/TM3,* Sb^{1} Ser^{1}	BDSC Stock #20915
Reporter lines			
1	*Stat92EGFP*	w^{1118};*10XStat92-EGFP*	(*30*)
2	*upd3-lacZ*	w^{1118}; *upd3-lacZ/Cyo*	(*67*)
3	*dad-lacZ*	w^{1118}; *dad-lacZ*	(*68*)
4	*diap1-GFP*	w^{1118}; *P{Diap1-GFP.3.5}/Cyo*	(*69*)
5	*TRE-DsRed*	w^{1118}; *P{TRE-DsRedT4}attP40*	BDSC Stock # 59012
6	*NRE-GFP*	w^{1118}; *P{NRE-EGFP.S}5A*	BDSC Stock # 30727
Mutant lines			
1	$upd1^{YM55}$	$w^{1118}upd1^{YM55}$*/FM7a*	BDSC Stock #4767
2	$upd2^{\Delta}$	w^{1118} $upd2^{\Delta}$	BDSC Stock #55727
3	$upd3^{\Delta}$	w^{1118} $upd3^{\Delta}$	BDSC Stock #55728
4	$prc^{MB03017}$	w^{1118}; $Mi\{ET1\}prc^{MB03017}$*/TM6C,* Sb^{1}	BDSC Stock #23836
UAS RNAi lines			

1	*UAS-statRNAi*	$y^1\ v^1$; *UAS-statRNAi*^{HMS00035}	BDSC Stock# 33637
2	*UAS-sar1RNAi*	$y^1\ sc^*\ v^1\ sev^{21}$;*UAS-sar1RNAi*^{HMS00355}/*TM3, Sb*^{1}	BDSC Stock #32364
3	*UAS-prcRNAi*	$y^1\ sc^*\ v^1\ sev^{21}$; *UAS-prcRNAi*^{HMC06160}	BDSC Stock #65898
4	*UAS-domeRNAi*	$y^1\ sc^*\ v^1\ sev^{21}$; *UAS-domeRNAi*^{HMS01293}	BDSC Stock #34618
5	*UAS-upd1RNAi*	$y^1\ sc^*\ v^1\ sev^{21}$; *UAS-upd1RNAi*^{HMS00545}	BDSC Stock #33680
6	*UAS-upd2RNAi*	$y^1\ sc^*\ v^1\ sev^{21}$; *UAS-upd2RNAi*^{HMS00901}	BDSC Stock #33949
7	*UAS-upd3RNAi*	$y^1\ sc^*\ v^1\ sev^{21}$; *UAS-upd3RNAi*^{HMS00646}	BDSC Stock #32859
8	*UAS-p38aRNAi*	$y^1\ sc^*\ v^1\ sev^{21}$; *UAS-p38aRNAi*^{HMS01224}	BDSC Stock #34744
9	*UAS-p38bRNAi*	$y^1\ sc^*\ v^1\ sev^{21}$; *UAS-p38bRNAi*^{GL00140}	BDSC Stock #35252
10	*UAS-p38cRNAi*	$y^1\ sc^*\ v^1\ sev^{21}$; *UAS-p38cRNAi*^{HMC05719}	BDSC Stock #64846
11	*UAS-kayRNAi*	$y^1\ sc^*\ v^1\ sev^{21}$; *UAS-kayRNAi*^{HMS00254}	BDSC Stock #33379
12	*UAS-foxoRNAi*	$y^1\ sc^*\ v^1\ sev^{21}$; *UAS-foxoRNAi*^{HMS00793}	BDSC Stock #32993
13	*UAS-ask1RNAi*	$y^1\ sc^*\ v^1\ sev^{21}$; *UAS-ask1RNAi*^{HMS00464}	BDSC Stock #32464
14	*UAS-noxRNAi*	$y^1\ sc^*\ v^1\ sev^{21}$; *UAS-noxRNAi*^{HMS00691}	BDSC Stock #32902
15	*UAS-duoxRNAi*	$y^1\ sc^*\ v^1\ sev^{21}$; *UAS-duoxRNAi*^{HMS00692}	BDSC Stock #32903
16	*UAS-notchRNAi*	$y^1\ v^1$; *UAS-notchRNAi*^{JF01637}	BDSC Stock #28981
17	*UAS-madRNAi*	$y^1\ v^1$; *UAS-madRNAi*^{JF01263}	BDSC Stock #31315
18	*UAS-yorkieRNAi*	$y^1\ v^1$; *UAS-ykiRNAi*^{JF03119}/*TM3, Sb*^{1}	BDSC Stock #31965
19	*UAS-sod1RNAi*	$y^1\ sc^*\ v^1\ sev^{21}$; *UAS-sod1RNAi*^{GL01016}	BDSC Stock #36804
20	*UAS-sod2RNAi*	$y^1\ v^1$; *UAS-sod2RNAi*^{JF01989}	BDSC Stock #25969
21	*UAS-catRNAi*	$y^1\ sc^*\ v^1\ sev^{21}$; *UAS-catRNAi*^{HMS00990}	BDSC Stock #34020

Table S2.

List of primers used:

For qPCR analysis		
Gene	**Primer Sequence**	
prc	**Forward**	AGAGGCTATTCGAGGGGACAA
	Reverse	GGAGCGAGATCCATTTTCGGTA
upd3	**Forward**	AGCCGGAGCGGTAACAAAA
	Reverse	CGAGTAAGATCAGTGACCAGTTC
rp49	**Forward**	CTAAGCTGTCGCACAAATGGC
	Reverse	TTCTGCATGAGCAGGACCTC

Supplementary Movies:

Movie S1.

Live imaging of the heart of w^{1118} adult fly.

Movie S2.

Live imaging of the heart of $prc^{MB03017}$/+ adult fly.

Movie S3.

Live imaging of the heart of *yolk-Gal4* adult fly.

Movie S4.

Live imaging of the heart of an adult fly upon knocking down *prc* in the fat body cells.

Movie S5.

Live imaging of the heart of an adult fly upon knocking down *sar1* in the fat body cells.

Movie S6.

Live imaging of the heart of *yolk-Gal4* adult fly.

Movie S7.

Live imaging of the heart of an adult fly upon knocking down *Stat92E* in the fat body cells.

Movie S8.

Live imaging of the heart of an adult fly upon over-expressing *Stat92E* in the fat body cells.

Movie S9.

Live imaging of the heart of $prc^{MB03017}$/+ adult fly upon overexpressing *Stat92E* in the fat body cells.

REFERENCES AND NOTES

1. A. Glasauer, N. S. Chandel, ROS. *Curr. Biol.* **23**, R100–R102 (2013).

2. C. L. Quinlan, I. V. Perevoshchikova, M. Hey-Mogensen, A. L. Orr, M. D. Brand, Sites of reactive oxygen species generation by mitochondria oxidizing different substrates. *Redox Biol.* **1**, 304–312 (2013).

3. W. Droge, Free radicals in the physiological control of cell function. *Physiol. Rev.* **82**, 47–95 (2002).

4. M. Schieber, N. S. Chandel, ROS function in redox signaling and oxidative stress. *Curr. Biol.* **24**, R453–R462 (2014).

5. T. Kietzmann, A. Gorlach, Reactive oxygen species in the control of hypoxia-inducible factor-mediated gene expression. *Semin. Cell Dev. Biol.* **16**, 474–486 (2005).

6. M. D. Buck, R. T. Sowell, S. M. Kaech, E. L. Pearce, Metabolic instruction of immunity. *Cell* **169**, 570–586 (2017).

7. T. F. Beckhauser, J. Francis-Oliveira, R. De Pasquale, Reactive oxygen species: Physiological and physiopathological effects on synaptic plasticity. *J. Exp. Neurosci.* **10**, 23–48 (2016).

8. Y. Higashi, S. Sasaki, K. Nakagawa, H. Matsuura, T. Oshima, K. Chayama, Endothelial function and oxidative stress in renovascular hypertension. *N. Engl. J. Med.* **346**, 1954–1962 (2002).

9. A. G. Toshniwal, S. Gupta, L. Mandal, S. Mandal, ROS inhibits cell growth by regulating 4EBP and S6K, independent of TOR, during development. *Dev. Cell* **49**, 473–489.e9 (2019).

10. A. Nugud, D. Sandeep, A. T. El-Serafi, Two faces of the coin: Minireview for dissecting the role of reactive oxygen species in stem cell potency and lineage commitment. *J. Adv. Res.* **14**, 73–79 (2018).

11. C. Dunnill, T. Patton, J. Brennan, J. Barrett, M. Dryden, J. Cooke, D. Leaper, N. T. Georgopoulos, Reactive oxygen species (ROS) and wound healing: The functional role of ROS and emerging ROS-modulating technologies for augmentation of the healing process. *Int. Wound J.* **14**, 89–96 (2017).

12. T. Finkel, The metabolic regulation of aging. *Nat. Med.* **21**, 1416–1423 (2015).

13. H. Huang, W. Du, R. A. Brekken, Extracellular matrix induction of intracellular reactive oxygen species. *Antioxid. Redox Signal.* **27**, 774–784 (2017).

14. E. Werner, Z. Werb, Integrins engage mitochondrial function for signal transduction by a mechanism dependent on Rho GTPases. *J. Cell Biol.* **158**, 357–368 (2002).

15. S. Honore, H. Kovacic, V. Pichard, C. Briand, J. B. Rognoni, Alpha2beta1-integrin signaling by itself controls G1/S transition in a human adenocarcinoma cell line (Caco-2): Implication of NADPH oxidase-dependent production of ROS. *Exp. Cell Res.* **285**, 59–71 (2003).

16. W. Sangrar, Y. Gao, M. Scott, P. Truesdell, P. A. Greer, Fer-mediated cortactin phosphorylation is associated with efficient fibroblast migration and is dependent on reactive oxygen species generation during integrin-mediated cell adhesion. *Mol. Cell. Biol.* **27**, 6140–6152 (2007).

17. K. Mori, T. Uchida, T. Yoshie, Y. Mizote, F. Ishikawa, M. Katsuyama, M. Shibanuma, A mitochondrial ROS pathway controls matrix metalloproteinase 9 levels and invasive properties in RAS-activated cancer cells. *FEBS J.* **286**, 459–478 (2019).

18. V. M. Chen, P. J. Hogg, Allosteric disulfide bonds in thrombosis and thrombolysis. *J. Thromb. Haemost.* **4**, 2533–2541 (2006).

19. S. Kaewpila, S. Venkataraman, G. R. Buettner, L. W. Oberley, Manganese superoxide dismutase modulates hypoxia-inducible factor-1 alpha induction via superoxide. *Cancer Res.* **68**, 2781–2788 (2008).

20. J. Myllyharju, E. Schipani, Extracellular matrix genes as hypoxia-inducible targets. *Cell Tissue Res.* **339**, 19–29 (2010).

21. N. Sampson, P. Berger, C. Zenzmaier, Redox signaling as a therapeutic target to inhibit myofibroblast activation in degenerative fibrotic disease. *Biomed. Res. Int.* **2014**, 131737 (**2014**).

22. J. L. Barnes, Y. Gorin, Myofibroblast differentiation during fibrosis: Role of NAD(P)H oxidases. *Kidney Int.* **79**, 944–956 (2011).

23. B. Rotstein, A. Paululat, On the morphology of the *Drosophila* heart. *J. Cardiovasc. Dev. Dis.* **3**, 15 (2016).

24. A. Chartier, S. Zaffran, M. Astier, M. Semeriva, D. Gratecos, Pericardin, a Drosophila type IV collagen-like protein is involved in the morphogenesis and maintenance of the heart epithelium during dorsal ectoderm closure. *Development* **129**, 3241–3253 (2002).

25. M. Drechsler, A. C. Schmidt, H. Meyer, A. Paululat, The conserved ADAMTS-like protein lonely heart mediates matrix formation and cardiac tissue integrity. *PLOS Genet.* **9**, e1003616 (2013).

26. A. C. Wilmes, N. Klinke, B. Rotstein, H. Meyer, A. Paululat, Biosynthesis and assembly of the Collagen IV-like protein Pericardin in *Drosophila melanogaster*. *Biol. Open* **7**, bio030361 (2018).

27. J. S. Bonifacino, B. S. Glick, The mechanisms of vesicle budding and fusion. *Cell* **116**, 153–166 (2004).

28. S. X. Hou, Z. Zheng, X. Chen, N. Perrimon, The Jak/STAT pathway in model organisms: Emerging roles in cell movement. *Dev. Cell* **3**, 765–778 (2002).

29. M. Amoyel, E. A. Bach, Functions of the Drosophila JAK-STAT pathway: Lessons from stem cells. *JAKSTAT* **1**, 176–183 (2012).

30. E. A. Bach, L. A. Ekas, A. Ayala-Camargo, M. S. Flaherty, H. Lee, N. Perrimon, G. H. Baeg, GFP reporters detect the activation of the Drosophila JAK/STAT pathway in vivo. *Gene Expr. Patterns* **7**, 323–331 (2007).

31. D. F. Eberl, L. A. Perkins, M. Engelstein, A. J. Hilliker, N. Perrimon, Genetic and developmental analysis of polytene section 17 of the X chromosome of *Drosophila melanogaster*. *Genetics* **130**, 569–583 (1992).

32. D. Osman, N. Buchon, S. Chakrabarti, Y. T. Huang, W. C. Su, M. Poidevin, Y. C. Tsai, B. Lemaitre, Autocrine and paracrine unpaired signaling regulate intestinal stem cell maintenance and division. *J. Cell Sci.* **125**, 5944–5949 (2012).

33. J. L. Chao, Y. C. Tsai, S. J. Chiu, Y. H. Sun, Localized Notch signal acts through eyg and upd to promote global growth in Drosophila eye. *Development* **131**, 3839–3847 (2004).

34. P. Houtz, A. Bonfini, X. Liu, J. Revah, A. Guillou, M. Poidevin, K. Hens, H. Y. Huang, B. Deplancke, Y. C. Tsai, N. Buchon, Hippo, TGF-β, and Src-MAPK pathways regulate transcription of the *upd3* cytokine in *Drosophila* enterocytes upon bacterial infection. *PLOS Genet.* **13**, e1007091 (2017).

35. P. Santabarbara-Ruiz, P. Santabárbara-Ruiz, M. López-Santillán, I. Martínez-Rodríguez, A. Binagui-Casas, L. Pérez, M. Milán, M. Corominas, F. Serras, ROS-induced JNK and p38 signaling is required for unpaired cytokine activation during *Drosophila* regeneration. *PLOS Genet.* **11**, e1005595 (2015).

36. E. Owusu-Ansah, A. Yavari, S. Mandal, U. Banerjee, Distinct mitochondrial retrograde signals control the G1-S cell cycle checkpoint. *Nat. Genet.* **40**, 356–361 (2008).

37. H. Y. Lim, W. Wang, J. Chen, K. Ocorr, R. Bodmer, ROS regulate cardiac function via a distinct paracrine mechanism. *Cell Rep.* **7**, 35–44 (2014).

38. Y. Sekine, R. Hatanaka, T. Watanabe, N. Sono, S. I. Iemura, T. Natsume, E. Kuranaga, M. Miura, K. Takeda, H. Ichijo, The Kelch repeat protein KLHDC10 regulates oxidative stress-induced ASK1 activation by suppressing PP5. *Mol. Cell* **48**, 692–704 (2012).

39. P. D. Ray, B. W. Huang, Y. Tsuji, Reactive oxygen species (ROS) homeostasis and redox regulation in cellular signaling. *Cell. Signal.* **24**, 981–990 (2012).

40. P. Niethammer, C. Grabher, A. T. Look, T. J. Mitchison, A tissue-scale gradient of hydrogen peroxide mediates rapid wound detection in zebrafish. *Nature* **459**, 996–999 (2009).

41. S. K. Yoo, T. W. Starnes, Q. Deng, A. Huttenlocher, Lyn is a redox sensor that mediates leukocyte wound attraction in vivo. *Nature* **480**, 109–112 (2011).

42. A. Hervera, F. de Virgiliis, I. Palmisano, L. Zhou, E. Tantardini, G. Kong, T. Hutson, M. C. Danzi, R. B. T. Perry, C. X. C. Santos, A. N. Kapustin, R. A. Fleck, J. A. del Río, T. Carroll, V. Lemmon, J. L. Bixby, A. M. Shah, M. Fainzilber, S. di Giovanni, Reactive oxygen species regulate axonal regeneration through the release of exosomal NADPH oxidase 2 complexes into injured axons. *Nat. Cell Biol.* **20**, 307–319 (2018).

43. M. Buggisch, B. Ateghang, C. Ruhe, C. Strobel, S. Lange, M. Wartenberg, H. Sauer, Stimulation of ES-cell-derived cardiomyogenesis and neonatal cardiac cell proliferation by reactive oxygen species and NADPH oxidase. *J. Cell Sci.* **120**, 885–894 (2007).

44. F. Zhang, Y. Zhao, Z. Han, An in vivo functional analysis system for renal gene discovery in Drosophila pericardial nephrocytes. *J. Am. Soc. Nephrol.* **24**, 191–197 (2013).

45. M. Helmstadter, T. B. Huber, T. Hermle, Using the Drosophila nephrocyte to model podocyte function and disease. *Front. Pediatr.* **5**, 262 (2017).

46. H. Y. Lim, H. Bao, Y. Liu, W. Wang, Select septate junction proteins direct ros-mediated paracrine regulation of Drosophila cardiac function. *Cell Rep.* **28**, 1455–1470.e4 (2019).

47. A. Sainio, H. Jarvelainen, Extracellular matrix-cell interactions: Focus on therapeutic applications. *Cell. Signal.* **66**, 109487 (2020).

48. B. Denholm, H. Skaer, Bringing together components of the fly renal system. *Curr. Opin. Genet. Dev.* **19**, 526–532 (2009).

49. H. Agaisse, U. M. Petersen, M. Boutros, B. Mathey-Prevot, N. Perrimon, Signaling role of hemocytes in Drosophila JAK/STAT-dependent response to septic injury. *Dev. Cell* **5**, 441–450 (2003).

50. H. Yang, J. Kronhamn, J. O. Ekstrom, G. G. Korkut, D. Hultmark, JAK/STAT signaling in Drosophila muscles controls the cellular immune response against parasitoid infection. *EMBO Rep.* **16**, 1664–1672 (2015).

51. S. Chakrabarti, J. P. Dudzic, X. Li, E. J. Collas, J. P. Boquete, B. Lemaitre, Remote control of intestinal stem cell activity by haemocytes in Drosophila. *PLOS Genet.* **12**, e1006089 (2016).

52. K. Huang, T. Miao, K. Chang, J. Kim, P. Kang, Q. Jiang, A. J. Simmonds, F. di Cara, H. Bai, Impaired peroxisomal import in Drosophila oenocytes causes cardiac dysfunction by inducing upd3 as a peroxikine. *Nat. Commun.* **11**, 2943 (2020).

53. K. J. Woodcock, K. Kierdorf, C. A. Pouchelon, V. Vivancos, M. S. Dionne, F. Geissmann, Macrophage-derived upd3 cytokine causes impaired glucose homeostasis and reduced lifespan in Drosophila fed a lipid-rich diet. *Immunity* **42**, 133–144 (2015).

54. L. A. Borthwick, T. A. Wynn, A. J. Fisher, Cytokine mediated tissue fibrosis. *Biochim. Biophys. Acta* **1832**, 1049–1060 (2013).

55. Y. X. She, Q. Y. Yu, X. X. Tang, Role of interleukins in the pathogenesis of pulmonary fibrosis. *Cell Death Discov.* **7**, 52 (2021).

56. Y. Kawaguchi, Contribution of interleukin-6 to the pathogenesis of systemic sclerosis. *J. Scleroderma Relat. Disord.* **2**, S6–S12 (2017).

57. G. C. Meléndez, J. L. Mc Larty, S. P. Levick, Y. Du, J. S. Janicki, G. L. Brower, Interleukin 6 mediates myocardial fibrosis, concentric hypertrophy, and diastolic dysfunction in rats. *Hypertension* **56**, 225–231 (2010).

58. E. H. Steen, X. Wang, S. Balaji, M. J. Butte, P. L. Bollyky, S. G. Keswani, The role of the anti-inflammatory cytokine interleukin-10 in tissue fibrosis. *Adv. Wound Care* **9**, 184–198 (2020).

59. D. D. Shao, R. Suresh, V. Vakil, R. H. Gomer, D. Pilling, Pivotal advance: Th-1 cytokines inhibit, and Th-2 cytokines promote fibrocyte differentiation. *J. Leukoc. Biol.* **83**, 1323–1333 (2008).

60. E. Owusu-Ansah, U. Banerjee, Reactive oxygen species prime Drosophila haematopoietic progenitors for differentiation. *Nature* **461**, 537–541 (2009).

61. M. Fink, C. Callol-Massot, A. Chu, P. Ruiz-Lozano, J. C. I. Belmonte, W. Giles, R. Bodmer, K. Ocorr, A new method for detection and quantification of heartbeat parameters in Drosophila, zebrafish, and embryonic mouse hearts. *Biotechniques* **46**, 101–113 (2009).

62. D. A. Kimbrell, C. Hice, C. Bolduc, K. Kleinhesselink, K. Beckingham, The Dorothy enhancer has Tinman binding sites and drives hopscotch-induced tumor formation. *Genesis* **34**, 23–28 (2002).

63. P. Georgel, S. Naitza, C. Kappler, D. Ferrandon, D. Zachary, C. Swimmer, C. Kopczynski, G. Duyk, J. M. Reichhart, J. A. Hoffmann, Drosophila immune deficiency (IMD) is a death domain protein that activates antibacterial defense and can promote apoptosis. *Dev. Cell* **1**, 503–514 (2001).

64. T. Sandmann, L. J. Jensen, J. S. Jakobsen, M. M. Karzynski, M. P. Eichenlaub, P. Bork, E. E. M. Furlong, A temporal map of transcription factor activity: Mef2 directly regulates target genes at all stages of muscle development. *Dev. Cell* **10**, 797–807 (2006).

65. S. A. Sinenko, T. Hung, T. Moroz, Q. M. Tran, S. Sidhu, M. D. Cheney, N. A. Speck, U. Banerjee, Genetic manipulation of AML1-ETO-induced expansion of hematopoietic precursors in a Drosophila model. *Blood* **116**, 4612–4620 (2010).

66. E. Kuranaga, H. Kanuka, T. Igaki, K. Sawamoto, H. Ichijo, H. Okano, M. Miura, Reaper-mediated inhibition of DIAP1-induced DTRAF1 degradation results in activation of JNK in Drosophila. *Nat. Cell Biol.* **4**, 705–710 (2002).

67. F. Zhou, A. Rasmussen, S. Lee, H. Agaisse, The UPD3 cytokine couples environmental challenge and intestinal stem cell division through modulation of JAK/STAT signaling in the stem cell microenvironment. *Dev. Biol.* **373**, 383–393 (2013).

68. K. Tsuneizumi, T. Nakayama, Y. Kamoshida, T. B. Kornberg, J. L. Christian, T. Tabata, Daughters against dpp modulates dpp organizing activity in Drosophila wing development. *Nature* **389**, 627–631 (1997).

69. L. Zhang, F. Ren, Q. Zhang, Y. Chen, B. Wang, J. Jiang, The TEAD/TEF family of transcription factor Scalloped mediates Hippo signaling in organ size control. *Dev. Cell* **14**, 377–387 (2008).